

# A Self-Powered, Real-Time, LoRaWAN IoT-Based Soil Health Monitoring System

S. R. Jino Ramson<sup>✉</sup>, Member, IEEE, Walter D. León-Salas<sup>✉</sup>, Member, IEEE, Zachary Brecheisen, Erika J. Foster, Cliff T. Johnston, Darrell G. Schulze, Timothy Filley, Rahim Rahimi<sup>✉</sup>, Senior Member, IEEE, Martín Juan Carlos Villalta Soto, Juan A. Lopa Bolívar, and Mauricio Postigo Málaga<sup>✉</sup>, Member, IEEE

**Abstract**—Typical soil health assessment requires intensive field sampling and laboratory analysis. Although this approach yields accurate results, it can be costly and labor intensive and not suitable for continuous tracking of soil properties. Advances in soil sensor and wireless technologies are poised to replace physical sampling and offline measurement with in-field monitoring. This article reports the development, deployment, and validation of an Internet-of-Things (IoT) system for continuous monitoring of soil health. The end nodes of the proposed system, called soil health monitoring units (SHMUs), are solar powered and can be installed on a field for extended periods of time. Each SHMU transmits soil temperature, moisture, electrical conductivity, carbon dioxide ( $\text{CO}_2$ ), and geolocation data wirelessly using long-range wide-area network (LoRaWAN) radio technology. Data are received by a LoRaWAN gateway, which uploads it to a server for long-term storage and analysis. Users can view acquired data through a Web-based dashboard. The following significant experiments were carried out to validate the developed system: 1) a network consisting of eight SHMUs was deployed at an agricultural field site for several weeks and soil health metrics were analyzed using the soil health dashboard; 2) the flexibility of the system was demonstrated by the addition of an extra  $\text{CO}_2$  sensor allowing an additional variable directly linked to soil health to be recorded; 3) a wireless communication range of 3422 m was estimated at a transmission power of 10 dBm by deploying the developed system on a large field; 4) the average current consumption of a SHMU (including its associated sensors) was estimated to be 13 mA, at this rate, the onboard Li-ion battery is able to sustain a SHMU for several days; and 5) a 7 cm × 6.5 cm solar panel was able to fully charge the onboard battery in 14 days while supplying power to the SHMU.

**Index Terms**—Agriculture, environmental monitoring, Internet of Things (IoT), long-range wide-area network (LoRaWAN), real-time systems, self-powered, sensor systems, soil measurements, solar power.

Manuscript received November 16, 2020; revised January 4, 2021; accepted January 27, 2021. Date of publication February 2, 2021; date of current version May 21, 2021. (Corresponding author: S. R. Jino Ramson.)

S. R. Jino Ramson is with the Department of Earth, Atmospheric, and Planetary Sciences and the School of Engineering Technology, Purdue University, West Lafayette, IN 47907 USA (e-mail: jinoramson@gmail.com).

Walter D. León-Salas is with the School of Engineering Technology, Purdue University, West Lafayette, IN 47907 USA.

Zachary Brecheisen, Cliff T. Johnston, and Darrell G. Schulze are with the Department of Agronomy, Purdue University, West Lafayette, IN 47907 USA.

Erika J. Foster and Timothy Filley are with the Department of Earth, Atmospheric, and Planetary Sciences, Purdue University, West Lafayette, IN 47907 USA.

Rahim Rahimi is with the Department of Materials Engineering, Purdue University, West Lafayette, IN 47907 USA.

Martín Juan Carlos Villalta Soto, Juan A. Lopa Bolívar, and Mauricio Postigo Málaga are with the Academic Department of Chemistry, National University of San Agustín of Arequipa, Arequipa 04012, Peru.

Digital Object Identifier 10.1109/JIOT.2021.3056586

## I. INTRODUCTION

**S**OIL is a natural body on the land surface consisting of solids, liquids, and gasses, that experiences “additions, losses, transfers, and transformations of energy and matter” [1]. Collectively, these dynamic soil processes affect “soil health,” defined as “the capacity of the soil to function as a vital living ecosystem that sustains plants, animals, and humans” [2]–[4].

Soil develops in response to forming factors of time, climate, organisms, topography, parent material, and human management [5], [6]. These soil-forming factors influence soil health, as measured through a combination of soil physical, chemical, and biological properties as shown in Fig. 1.

### A. Soil Health Monitoring

Soil health monitoring can encompass many metrics that help to quantify soil function and specific ecosystem services. Typically, soil health measurements involve intensive field sampling and costly laboratory analysis. However, the laboratory analysis can often only incorporate samples at a coarse spatial and temporal resolution, the resulting data cannot provide dynamic tracking of critical biophysical properties to support management decisions on a fine timescale [7].

In addition, tracking soil health for effective land management must occur at regular intervals and at multiple locations to capture multiple sources of variation at different scales. Variation in soil health stems from temporal variability (e.g., daily weather, growing season, and climate), spatial heterogeneity (e.g., rooting zone, changes in depth, crop rows, surface topography, and watershed dynamics), and management practices (e.g., local fertilizer application, and type of tillage). Due to scaling issues, numerous sources of variability, and high costs, the development of inexpensive *in situ* monitoring system with master control over physical, chemical, and biological metrics is required.

Technological advances in environmental sensors and data loggers allow continuous data collection to inform management decisions [8]. Previous instrumentation and deployment of high-quality soil sensors with data loggers across space and at depth can be cost prohibitive, and even impossible to connect via the Internet or cellular networks in remote areas [9].

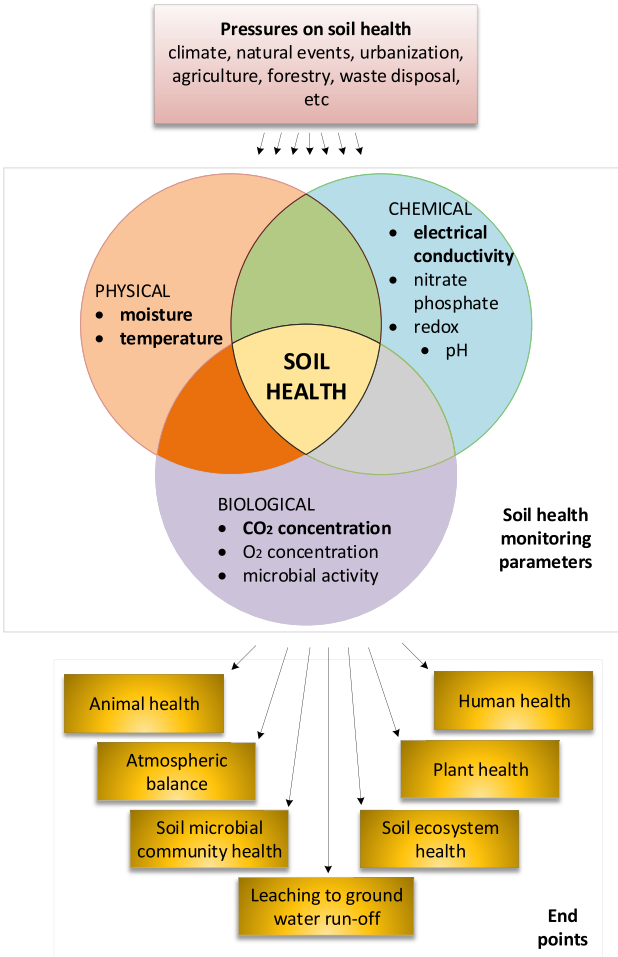


Fig. 1. Conceptual representation of the three types of soil properties critical to a healthy soil. Monitoring requires measurements within all of these categories. Bold metrics are currently included in the proposed system.

### B. IoT-Based Remote Monitoring Systems

Nevertheless, presently available microelectronics, lightweight communication protocols, opensource servers, visualization dashboards, and Web development tools make the Internet of Things (IoT) a promising approach for remote monitoring [10]–[12]. Several IoT-based remote monitoring systems have been employed in various disciplines, such as athlete monitoring in challenging cycling environments [13], machine vibration monitoring [14], physical fitness monitoring [15], pain monitoring system [16], nitrate monitoring [17], trash bin level monitoring system [18], health monitoring systems [19], [20], and so on. This article presents the development, deployment, and validation of an IoT system to monitor the dynamic soil properties in real time and to ease data collection in remote field sites.

### C. Features of the Proposed System

The main features of the developed IoT-based soil health monitoring (IoT-SHM) system are as follows: a flexible platform that allows seamless addition of sensors with different types of interfaces to monitor physical, chemical, and biological properties of soil; long-range data transmission to cover

large tracts of land; scalable in a plug-and-play fashion; solar energy harvesting with maximum power point tracking and battery charging; multiple power options (3.3, 5, and 12 V) for sensors; geolocation of sampling points; long-time data storage and a dashboard for data visualization and analysis; battery undervoltage and overvoltage protection, and battery status indicator; expansion board to connect additional sensors; downlink channel for feedback control.

The remainder of this article is organized as follows. In Section II, the current state-of-the-art is discussed and Section III describes the design of the proposed IoT-SHM system. The design includes selection of the network architecture, design of soil health-monitoring units (SHMUs), and set up of a LoRa gateway and an IoT-SHM server. In Section IV, the experimental results are discussed. The experimental results include the deployment and testing of the proposed system in an agricultural field, soil health analysis, measurement of wireless range, average current consumption, battery charging time, implementation cost, and summary of results. Section V concludes this article.

## II. RELATED WORK

Soil health has been investigated for many decades through expensive laboratory analysis. In order to overcome the limitations of laboratory analysis, field sampling systems were introduced. Although many interacting processes affect soil health, the established field monitoring systems focus on only few key properties, such as soil moisture, temperature, and electrical conductivity (EC). These three common measurements interact and control many dynamic biogeochemical processes in the soil [21].

For example, soil moisture diffuses the substrate to the nutrient cycling bacteria and fungi and, thus, the water content ultimately controls the dominant type of metabolism (broadly, aerobic or anaerobic), altering soil biology. To track changes in soil microbial cycling, newly developed field sensors precisely measure microbial and root respiration of CO<sub>2</sub> [22], [23]. All of these dynamic soil properties can serve as indicators of soil health and their interactions can be monitored *in situ* at spatially and temporally relevant scales [3].

To monitor soil health in the temporal resolution and spatial resolution, advanced data loggers and sensors were introduced. Temporal resolution on a subdaily interval across a growing season can inform management practices, such as the timing of irrigation and fertilization [24]. Maintaining robust sensors over longer time periods can track seasonal changes relevant to planting and harvest times in agriculture or native soil restoration projects. Increasing spatial resolution across a site using multiple sensors at various depths can delineate management zones (e.g., [25]), monitor remediation progress (e.g., [26]), or promote agricultural efficiency through precision agricultural practices (e.g., [27]). However, the deployment of high-quality soil sensors with data loggers across space and at depth can be cost prohibitive, and even impossible to connect via the Internet or cellular networks in remote areas.

**TABLE I**  
COMPARISON OF THE EXISTING SOIL HEALTH MEASUREMENT SYSTEMS

Ref. & Year	Soil parameters	Wireless connectivity	Network type	Energy harvesting	GPS	Storage	Visualization	Down-link channels for feedback control
[29], 2010	Moisture	ZigBee	WPAN	No	No	Yes	No	No
[30], 2012	Snow depth Moisture Solar radiation Temperature	ZigBee	WPAN	No	No	Yes	No	No
[31], 2013	Temperature Light	ZigBee	WPAN	No	No	Yes	Yes	No
[32], 2013	Nil	TI CC1150	WLAN	No	No	Yes	Yes	No
[33], 2014	Temperature Light Moisture	ZigBee	WPAN	No	No	Yes	No	No
[34], 2014	Moisture	ZigBee	WLAN	Yes	No	Yes	No	No
[35], 2015	CO <sub>2</sub>	ZigBee	WLAN	No	No	Yes	No	No
[36], 2017	Moisture Temperature Light	ZigBee	WLAN	No	No	Yes	No	No
[37], 2017	Water potential Moisture	ZigBee	WLAN	No	No	Yes	Yes	No
[38], 2017	Temperature Moisture pH	Wi-Fi	WLAN	No	No	No	No	No
[39], 2018	Temperature Moisture EC	ZigBee	WLAN	Yes	No	Yes	Yes	No
[40], 2019	Moisture	ZigBee	WLAN	No	No	No	No	No
[41], 2019	Moisture	Wi-Fi	WLAN	No	No	Yes	No	No
[42], 2018	pH Moisture	LoRaWAN	WWAN	No	No	Yes	Yes	No
[43], 2018	Temperature Moisture	LoRa	WWAN	No	No	No	No	No
[44], 2020	Temperature pH Turbidity Dissolved oxygen EC Water level	LoRaWAN	WWAN	No	No	No	No	No
[45], 2020	Moisture	RFID & LoRa	WWAN	No	No	Yes	No	No
Proposed system	Temperature Moisture EC CO <sub>2</sub>	LoRaWAN	WWAN	Yes	Yes	Yes	Yes	Yes

#### A. Wireless Sensor Network, and IoT-Based Soil Health Measurement Systems

The wireless sensor network (WSN) and IoT-based monitoring systems ensure low cost, high fidelity, flexibility, and rapid deployment [28]. A comparison of the existing soil health measurement systems [29]–[45] in terms of wireless connectivity and features are listed in Table I. Most of these systems rely

on ZigBee and Wi-Fi wireless technologies to transmit sensor data.

A comparative study of wireless technologies in terms of the wireless range and power usage is presented in [46]. This study shows that wireless technologies, such as ZigBee, Bluetooth, Wi-Fi, IEEE 802.11p, DSRC/WAVE, DASH7, and 6LoWPAN have relatively short-communication range. A solution to

increase the communication range of these wireless technologies is the adoption of a wireless mesh network topology. However, the mesh network topology requires additional coordinator nodes to route data to a sink node, increasing the cost of the network. In addition, mesh networks exhibit a rapid increase in complexity and power consumption as the network scales up [47].

On the other hand, the long-range wide-area network (LoRaWAN), SIGFOX, and NB-IoT wireless networking protocols can achieve long communication range (in the order of kilometers) while consuming low power and without the need for intermediate nodes. These features make LoRaWAN, SIGFOX, and NB-IoT networks very attractive for agricultural applications [48], [49]. However, NB-IoT requires an expensive dedicated regional frequency/channel, and SIGFOX is a proprietary network and protocol. Nevertheless, LoRaWAN is an open specification. Therefore, anyone can implement this networking protocol free of cost.

### B. LoRa/LoRaWAN-Based Soil Health Monitoring Systems

Some soil health measurement systems based on LoRa/LoRaWAN networking have been reported so far in [42]–[45]. A design of a LoRa-based IoT monitoring system for starfruit plantation is presented in [42]. The end nodes of this system use an Arduino Uno board to interface a pH sensor and a soil moisture sensor to monitor soil health. In addition, a Dragino shield was used to interface a LoRa module with the Arduino Uno board. Each sensor node measures soil parameters and uploads them to a server through a single channel gateway. This system achieved a communication range of 700 m with a packet delivery ratio of 40.9%. In [43], a custom information monitoring system based on the LoRa networking protocol is presented. The main advantage of this system is the combination of LoRa and NB-IoT technology to increase the data transmission range. Each end node employs the LoRa protocol to transmit data to a gateway. The gateway is interfaced with an NB-IoT module to transmit data to a remote location through the Internet. Experimental results show a maximum communication range between an end sensor node and a gateway of 1.6 km. Moreover, as the gateway relies on cellular networks, it will be difficult to deploy it in remote field sites.

A LoRa-based wetland monitoring system is presented in [44]. The end nodes of this system consist of six sensors, namely, water temperature sensor, pH sensor, turbidity sensor, dissolved oxygen sensor, conductivity sensor, and a water-level sensor. The end node collects data from the sensors and sends them to a gateway, which uploads them to a server. No measurement results were provided on the transmission range, power consumption, life expectancy, and data visualization. Recently, an RFID and LoRa technology-based soil health monitoring system is presented in [45]. This monitoring system includes a patrol car, RFID sensors, and a storage platform. An RFID reader and a LoRa module were mounted on the patrol car, which was responsible for collecting data from embedded RFID sensors and transmitting them

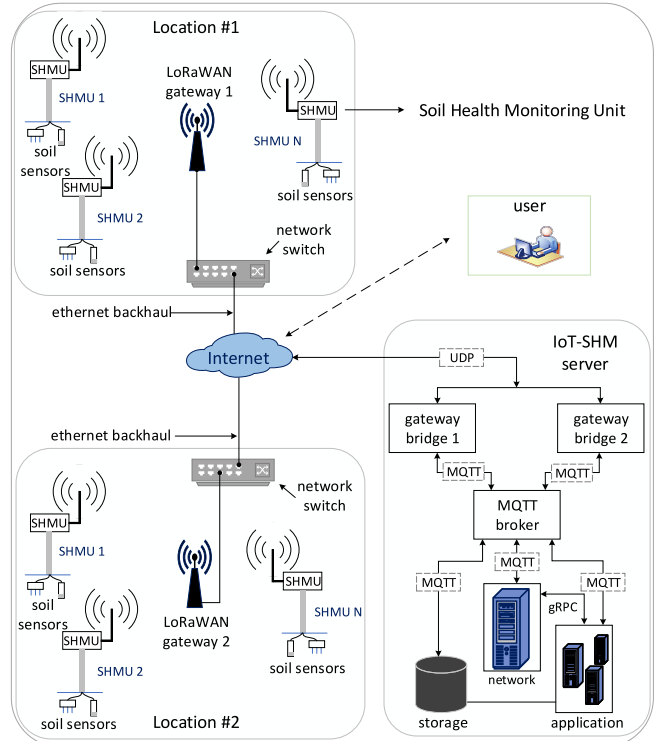


Fig. 2. Network architecture of the proposed IoT-SHM system.

to a monitoring station. A drawback of this system is that it requires a patrol car and manpower to collect data.

Most soil scientists and agricultural producers prefer low-cost flexible platforms that allow seamless addition of sensors with different types of interfaces to measure the physical, chemical, and biological properties of soil, ease to scale, have long communication range, and have some form of ambient energy harvesting capability to reduce the burden of battery recharging or replacement. Other desirable features include geolocation of sampling points, long-term data storage, dashboard for data visualization, and a downlink channel for possible feedback control. A review of the published work on soil health monitoring systems summarized in Table I shows that such a system has not been built before. Therefore, we developed a self-powered, ruggedized, scalable, IoT-based soil health monitoring system. The design and test of this system are reported here.

## III. DESIGN OF THE IOT-SHM SYSTEM

### A. Network Architecture of the Proposed IoT-SHM System

The IoT-SHM system employs the LoRaWAN architecture.<sup>1</sup> In this architecture, a network is deployed in a star-of-stars topology as shown in Fig. 2. The end nodes of the proposed system, called SHMUs, are deployed at every location to collect soil-related variables (temperature, EC, moisture, and CO<sub>2</sub>) and location data, and after processing them, transmit them to a LoRaWAN gateway using the 900-MHz ISM radio band. The wireless communication between a SHMU and a LoRaWAN gateway is a single-hop link that takes advantage of

<sup>1</sup><https://lora-alliance.org/>

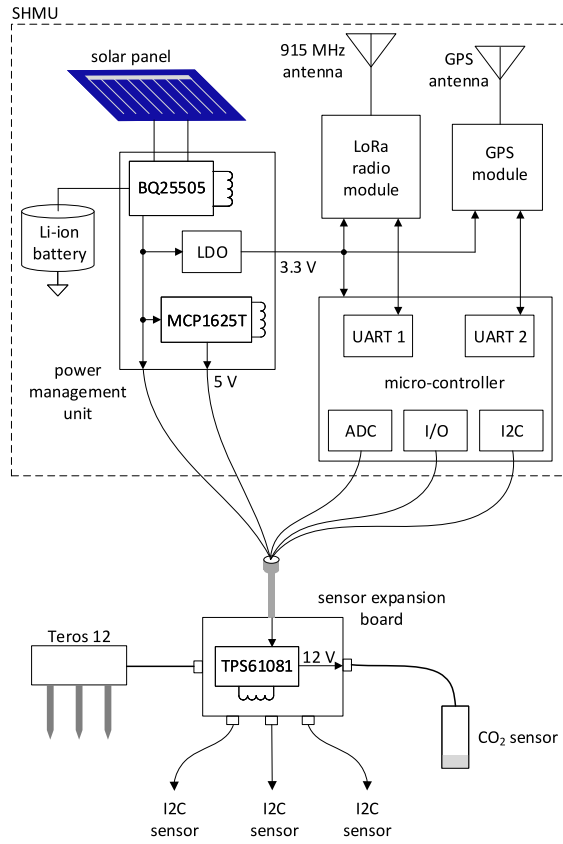


Fig. 3. Block diagram of the SHMU with the sensor expansion board.

the long-range characteristics of the LoRa physical layer. The LoRAWAN gateways connect to the Internet via a network switch and from there to a central IoT-SHM server. The LoRaWAN gateways serve as a concentrator for the SHMUs, and relay data between the SHMUs and the central IoT-SHM server.

#### B. Soil Health-Monitoring Unit

A SHMU consists of soil sensors, a host microcontroller, a LoRa radio module, a GPS module, a 7 cm × 6.5 cm solar cell (MIKROE-651), a 2500-mAh Li-ion battery, a power management unit to charge the battery and provide a stable supply voltage. A block diagram of the SHMU is portrayed in Fig. 3 and the populated printed circuit board of a SHMU is shown in Fig. 4. A sensor expansion board allows multiple sensors to be connected to the SHMU is shown in Fig. 5. The sensor expansion board supports three analog inputs, three SDI-12 serial ports, and up to six sensors with I2C interface. It also incorporates a boost dc-dc converter (TPS61081 from Texas Instruments) that generates 12 V to supply power to sensors. A fabricated SHMU prototype (main board with an IP67 enclosure) is shown in Fig. 6.

**1) Soil Sensors:** Our system uses two main sensors: 1) the Teros 12, a commercially available soil sensor from Meter Group and 2) the GMP251, a CO<sub>2</sub> sensor from Vaisala. The Teros 12 is a high-end soil sensor capable of measuring soil temperature, EC, and moisture. The Teros 12 sensor comes

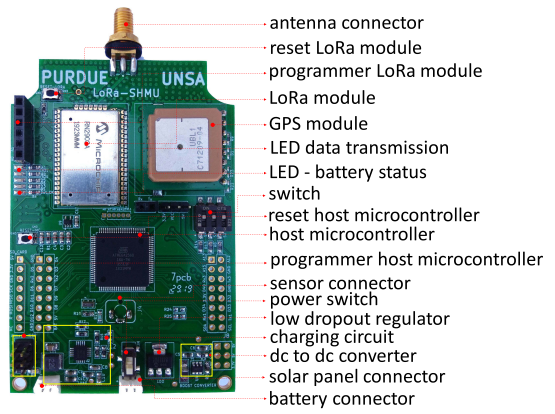


Fig. 4. Populated printed circuit board of a SHMU.

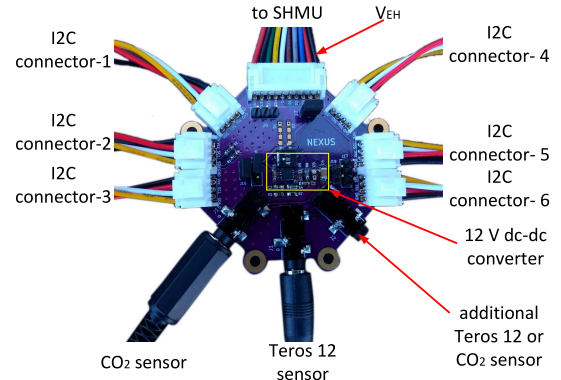


Fig. 5. Populated printed circuit board of a sensor expansion board.

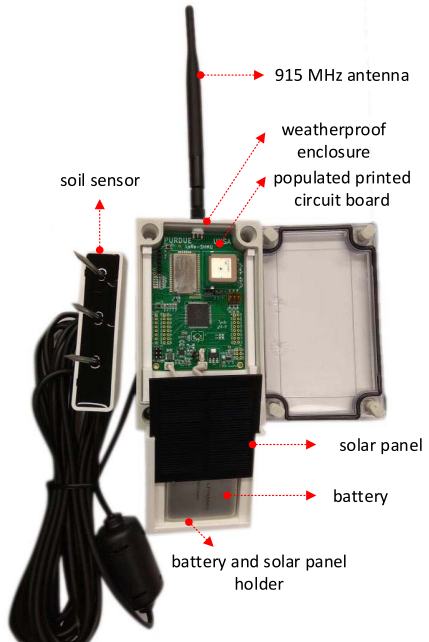


Fig. 6. Fabricated SHMU prototype with a Teros 12 sensor.

precalibrated for mineral soil and has the following specifications: volumetric water ranges from 0 to 0.70 m<sup>3</sup>/m<sup>3</sup> with a resolution of 0.001 m<sup>3</sup>/m<sup>3</sup>, temperature ranges from -40 °C to 60 °C with a resolution of 0.1 °C, and bulk EC ranges

from 0 to 10 dS/m with a resolution of 0.001 dS/m. Other features of the Teros 12 sensor are reduced sensor-to-sensor variability, extremely ruggedized epoxy fill designed to last up to ten years in the field, and stainless steel needle probes for easy installation in soil. Moreover, the Teros 12 sensor consumes low power (3.6 mA in active mode and 0.03 mA in sleep mode). These features make the Teros 12 very attractive for long-term soil health monitoring.<sup>2</sup> The Teros 12 receives power (5 V) from the power management unit and interfaces with the host microcontroller through a SDI-12 port.

The Vaisala GMP 251 sensor is a nondispersive infrared sensor and was chosen specifically because it is constructed to withstand a wide range of environmental conditions including a temperature range from  $-40^{\circ}\text{C}$  to  $60^{\circ}\text{C}$  and a measurement range from 0% to 20%. This sensor also includes a heater to prevent condensation and is housed inside an IP65-rated enclosure.<sup>3</sup> Furthermore, the Vaisala GMP 251 is able to operate in below ground soil installations. The GMP 251 CO<sub>2</sub> sensor has an analog output, which is read using the analog-to-digital converter (ADC) embedded in the host microcontroller.

2) *Host Microcontroller*: The host microcontroller is the ATmega 2560 from Atmel. It is responsible for controlling and coordinating all the functions of the SHMU. The flow diagram of a firmware running on the host-microcontroller to control the SHMU is shown in Fig. 7. This microcontroller was chosen due to its rich set of peripherals which include a 16-channel 10-b ADC, four UARTs, SPI and I2C serial interfaces, several counters, and an analog comparator. This microcontroller also features a low-power core, which consumes 500  $\mu\text{A}$  in active mode and 0.1  $\mu\text{A}$  in power-down mode.<sup>4</sup>

3) *Radio Module and Wireless Communications*: Each SHMU uses the RN2903 LoRa radio module. The RN2903 module uses spread spectrum modulation to achieves high interference immunity. The RN2903 has a sensitivity of  $-146$  dBm and an adjustable transmission power of up to 18.5 dBm. Furthermore, it can be configured and controlled using ASCII commands over a UART port. The RN2903 consumes 124 mA while transmitting at maximum power and 13.5 mA in reception mode. Before a SHMU can start sending soil and location data, it must join the IoT-SHM server using a process called over-the-air activation (OTAA). During this process, the RN2903 exchanges a series of messages with the IoT-SHM server leading to the creation of an encrypted communication link. After this secure communication link is established, the SHMU sends the soil and location data.

4) *Power Management Unit*: The power management module consists of an energy harvesting and battery charging integrated circuit (BQ25505 from Texas Instruments), a dc-to-dc converters (MCP16252T from Microchip) to generate 5 V, and a low-dropout (LDO) regulator (MCP1825S from Microchip) to generate 3.3 V. The BQ25505 has many features that make it attractive for self-powered sensors. For instance, it can draw power from a solar cell with an output voltage as low as 100 mV, it can track the solar cell's maximum power point

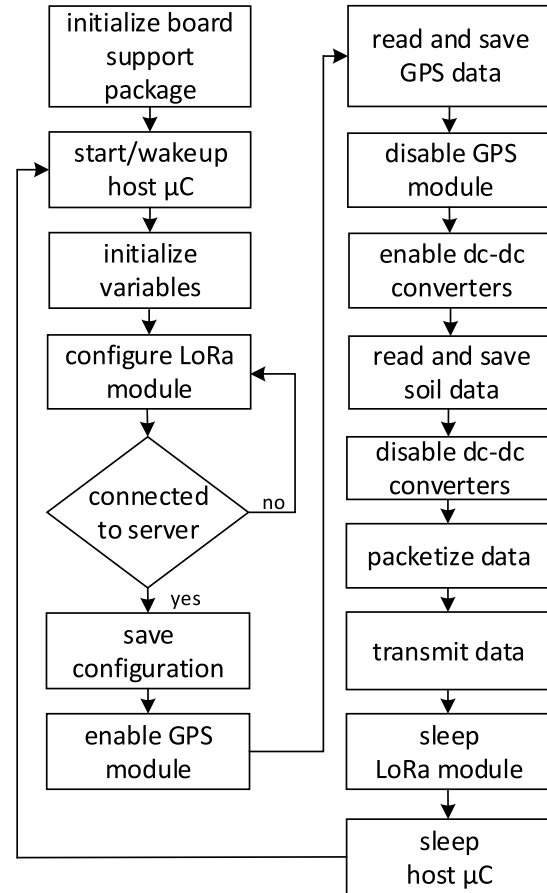


Fig. 7. Flow diagram of the firmware running on the host-microcontroller.

and has internal protection circuits to prevent deep discharge and damage to the battery. The supply voltages generated by the power management unit are used to meet the power requirements of the different sensors and circuits connected to a SHMU. For instance, the 5-V supply powers the Teros 12 sensor while the 3.3-V supply powers the GPS module, the LoRa radio, and the host microcontroller. The power management unit also outputs the battery voltage  $V_{EH}$  that is fed to the boost dc-dc converter in the sensor expansion board.

5) *GPS Module*: When soil health is being monitored in a wide area, multiple SHMUs need to be installed. The location of each SHMU (sampling point) is necessary to spatially analyze soil health by generating soil maps across a landscape. Although positioning solutions for sensor networks based on multilateration have been proposed and demonstrated, positioning based on GPS exhibits higher accuracy in outdoor scenarios [50]. Due to this advantage, the location of each SHMU is measured by an onboard GPS module. The onboard GPS module allows seamless and continuous geolocation of sensors even if a SHMU is relocated. The relocation of soil sensors in an agricultural field is needed during the planting and harvest seasons or when changes to the field, such as the installation on new irrigation lines, are introduced. The GPS module used in the SHMU features an embedded antenna, high sensitivity ( $-161$  dBm), and interference suppression.<sup>5</sup>

<sup>2</sup>Meter-Group, Teros 11/12 User Manual, 2018.

<sup>3</sup>Vaisala, Carbon Dioxide Probe GMP251 User Guide, 2018, rev. 3.

<sup>4</sup>Microchip, ATmega640/V-1280/V-1281/V-2560/V-2561/V, 2020.

<sup>5</sup>U-blox, PAM-7Q GPS Antenna Module, 2015, rev. 5.

TABLE II  
COMPONENTS OF THE SHMU AND THEIR FUNCTIONS

Component	Function
Soil sensors: Teros 12 and GMP251	Teros 12 : Measures soil temperature, moisture and EC. GMP251 : Measures soil CO <sub>2</sub> .
Host micro-controller: Atmega 2560	Controls and coordinates all the functions of the SHMU.
Radio module: RN2903	Transmits data to a long distance with low power.
GPS module: PAM-7Q	Measures the geo-location of a sampling point.
Power management unit: BQ25505, MCP16252T and MCP1825S.	BQ25505: Harvests solar energy and charges the battery. MCP16252T: A DC-to-DC converter to power up the Teros 12 sensor. MCP1825S: A LDO to power up the host micro-controller, radio module and GPS module.
Solar panel: MIKROE-651	Transforms energy into electricity from the sun.
Li-ion battery: 2500 mAh	Stores energy.

The GPS module communicates with the host microcontroller through a UART port. To reduce the overall SHMU's average power consumption, the GPS module is periodically placed in the power-save mode by the host microcontroller.

A summary of the components of the SHMU and their functions is summarized in Table II.

### C. LoRaWAN Gateway

To provide wireless connectivity between the IoT-SHM server and several SHMUs, the IoT-SHM system uses a commercially available LoRaWAN gateway from Microchip. The LoRaWAN gateway hardware employs the SX1301 radio chip from Semtec, which is specifically designed to offer breakthrough gateway capabilities in the outdoor environment. The gateway consists of eight parallel received channels with a sensitivity of  $-142.5$  dBm and ten programmable parallel demodulation paths. The data packets received by the gateway are forwarded to the IoT-SHM server through an Ethernet port. The software running on the LoRaWAN gateway responsible for receiving and sending messages to the IoT-SHM server is called the packet forwarder.

### D. IoT-SHM Server

The IoT-SHM server physically runs on a personal computer with an Intel Core i7-9700T (8 Cores/12 MB/8T/2.0 GHz to 4.3 GHz/35 W) processor, 16-GB RAM, 500-GB hard drive running the Ubuntu 18.04 LTS operating system. The software package of the IoT-SHM server consists of opensource programs, such as ChirpStack, Mosquitto, and PostgreSQL. The ChirpStack consists of different software components, such as the ChirpStack network server, ChirpStack gateway bridge, and ChirpStack application server. The Mosquitto

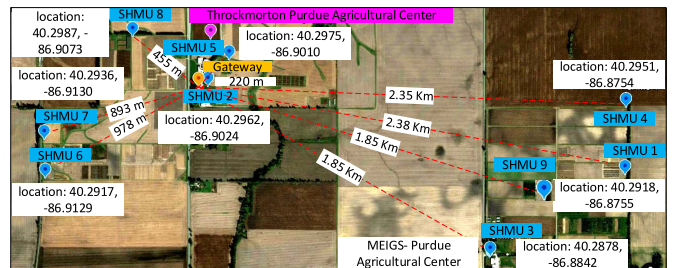


Fig. 8. Map showing the location of SHMUs and the distance between SHMUs and the LoRa gateway in the field site (Throckmorton Purdue Agricultural Center).

message broker implements the message queuing telemetry transport (MQTT) protocol to carry data using a publish/subscribe model between the ChirpStack gateway bridge and the ChirpStack network server.

The ChirpStack network server implements the LoRaWAN network. This server eliminates duplicate packets, manages security, and the scheduling of downlink frames and data rates. The ChirpStack gateway bridge is a service that serves as an interface between the LoRaWAN gateway packet forwarder and the Mosquitto message broker. It receives messages from the LoRaWAN gateway (UDP packets) and translates them to the JSON data format. The ChirpStack application server is responsible for handling the join process of SHMUs and decoding the application payload. Once data are decoded, the payload is pushed to PostgreSQL for long-time data storage and visualization.

## IV. EXPERIMENTAL EVALUATION

### A. Deployment and Testing of the Developed System

The developed IoT-SHM system was deployed and tested at the Throckmorton Purdue Agricultural Center (TPAC). TPAC is located in Lafayette, Indiana (Lat: 40.296, Lon:  $-86.903$ ) and consists of about 336 hectares in which 30 different crops are grown. A weather station measuring the air temperature, solar radiation, and precipitation is available at TPAC. The deployed IoT-SHM system comprises nine SHMUs (scalable in a plug-and-play fashion), a LoRaWAN gateway, and an IoT-SHM server. The location of the LoRaWAN gateway and the SHMUs, and the distance between SHMUs and the LoRaWAN gateway are shown in Fig. 8. The antenna employed for the LoRa gateway is an omnidirectional dipole antenna with a gain of 2 dBi. It was installed vertically on the roof of a nearby building at a height of 7.9 m from the ground. The installation of the antenna, LoRa gateway, and the network switch, which connects the gateway to the Internet, is shown in Fig. 9.

Eight SHMUs (SHMU 1–SHMU 8) each with a Teros 12 sensor were deployed at the TPAC site to record soil temperature, EC and moisture. The deployment of a SHMU with a Teros 12 sensor is shown in Fig. 10. The Teros 12 soil sensors were installed at the depth of 10 cm with their needle electrodes aligned horizontally (body-oriented vertically) to provide the minimum restriction to soil water flow as shown

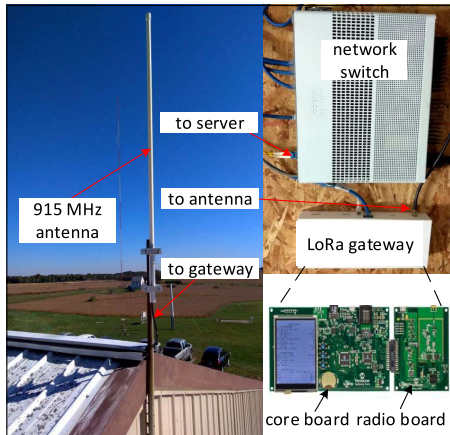


Fig. 9. Deployment of 915-MHz omnidirectional antenna on the roof of a building, LoRaWAN gateway and the network switch (Cisco Catalyst 3560-cx) are installed inside the building.

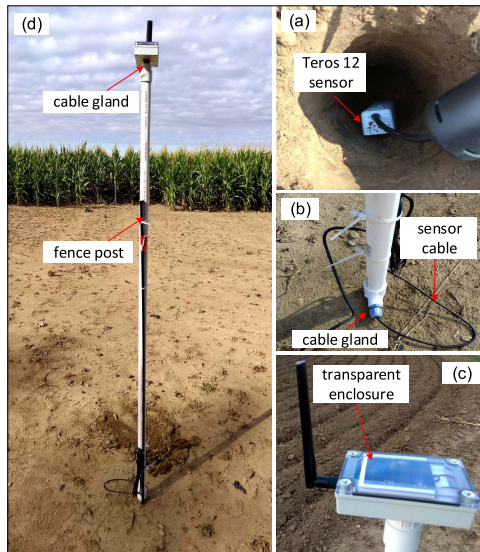


Fig. 10. Deployment of a SHMU with a Teros 12 sensor at the depth of 10 cm to monitor soil temperature, moisture, and EC. (a) Installation of a Teros 12 sensor with electrodes aligned horizontally (body oriented vertically). (b) Installation of sensor cable and the cable gland to protect from moisture. (c) Top view showing the installation of weather-proof transparent enclosure. (d) Full view of a SHMU.

in Fig. 11. Also, installing the sensor body oriented vertically integrates more soil depth into the measurement of soil moisture due to the shape of the sensor's electromagnetic field.

The SHMUs were configured to send soil measurements to the IoT-SHM server every 10 min. At the IoT-SHM server, these measurements were recorded for long-term storage and visualized in real time using the soil health-monitoring dashboard shown in Fig. 12. The soil health-monitoring dashboard displays the soil moisture, soil EC, and soil temperature data from the SHMUs in separate time-series charts. It also displays the latest value of soil moisture, soil EC, and soil temperature for every SHMU in separate widgets to help soil scientists and land managers evaluate soil parameters efficiently.

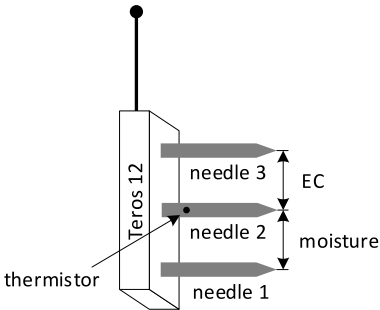


Fig. 11. Recommended deployment position of a Teros 12 sensor.

Soil temperature, moisture, and EC were recorded for 11 days (December 28–January 7). Fig. 13 shows the data collected along with air temperature measured by the weather station at TPAC. All the measured values fell within expected ranges for the field site [51], [52]. Soil temperature ranged between 1.2 °C and 11.3 °C, with an average of 2 °C over the measurement period. The SHMUs captured typical soil temperature dynamics, apparent in the lag time observed between the air temperature maximum 16.0 °C on December 29, and surface soil temperature recorded the maximum value 11.3 °C on December 30.

Similarly, for soil moisture, the SHMUs captured values from 24.7% to 30.1% volumetric soil moisture, with an average of 26.6% soil moisture over the 11-day period as shown in Fig. 13(b). The sensors captured the expected influence of topography on soil moisture, as the Teros 12 inserted within a low point at the research station (SHMU 7) shows greater soil moisture persistence, as expected and modeled by soil scientists [53], [54]. As expected, the soil moisture increased an average of 1.9% across all the sensors after rainfall events (e.g., rainfall on December 29 of 15.7 mm and December 30 of 24.12 mm). This rainfall event also impacted the soil EC which is shown in Fig. 13(c). After the first rainfall event (December 29), the EC increased by 3.47 dS/m averaged over all of the sensors. Again, this pattern occurs in clayey nonsaline soils (< 4 dS/m) due to the higher EC of moist versus dry soil. In this ecosystem, higher soil moisture leads to higher EC [55], [56]. A final interesting pattern in the data was the relatively high EC at site 6 (SHMU 6). The average EC of 3.7 dS/m over the sampling period could result from a higher clay content and, perhaps, even the slightly higher soil moisture at this site (27.7% on average).

### B. Soil Health Analysis

Biological parameters, such as CO<sub>2</sub>, O<sub>2</sub>, and microbial activities play a key role in determining soil health [57]. In order to evaluate the potential for the expansion of the IoT-SHM system and to capture a soil health variable directly linked to biological signaling, we added a Vaisala GMP251 CO<sub>2</sub> sensor to a SHMU (SHMU 9) alongside a Teros 12 sensor. Analog voltage output was used for this testing as it illustrates the adaptability of the SHMU platform to accept a wide variety of sensors on the market and even new sensors under development. The period of testing was from February



Fig. 12. Data collected over 21 days for three measurements of soil health displayed in the soil health monitoring dashboard. The soil health-monitoring dashboard displays the soil moisture, soil EC, and soil temperature of all the SHMUs in a separate time-series chart. Also, it displays the latest value of soil moisture, soil EC, and soil temperature of all the SHMUs in separate widgets.

14 to February 19, 2020 at the TPAC site. The CO<sub>2</sub> sensor was installed approximately 35 cm below the soil surface and inside a protective white PVC chamber. The sensor was

installed at approximately 2 m from an evergreen pine tree as shown in Fig. 14. The proximity to an evergreen tree was desired because this testing was conducted during winter, a

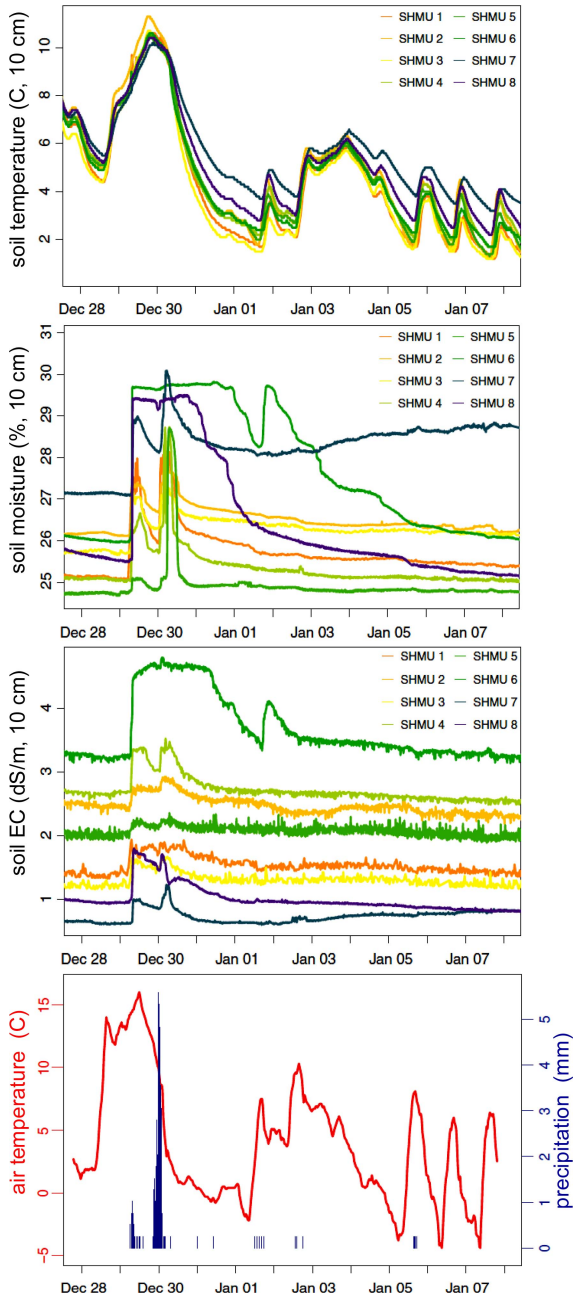


Fig. 13. Soil health metrics collected over 11 days. (a) Soil temperature. (b) Soil moisture. (c) Soil EC. (d) Air temperature and precipitation from the TPAC weather station.

time when the annual crops were absent from agricultural fields and local deciduous trees were dormant. Aboveground dormancy or absence of vegetation is reflected in low below-ground respiration dynamics [22], [23]. Therefore, the CO<sub>2</sub> sensor was installed in proximity to the Teros 12 sensor. The Teros 12 sensor was installed in a separate bore hole approximately 10 cm below the soil surface adjacent to the CO<sub>2</sub> sensor.

Over the testing period, we were able to observe several environmental phenomena as well as the interaction of above and belowground processes. In Fig. 15, over the first 12 h of observation, we can see the process of re-equilibration of



Fig. 14. Deployment of a CO<sub>2</sub> sensor approximately 35 cm below the soil surface and inside a protective PVC chamber (enclosure). The sensor was deployed at approximately 2 m from an evergreen pine tree.

soil CO<sub>2</sub> concentration occurring as it rose rapidly from ambient aboveground concentration of 0.04% to 0.5%. Data from this period would not be used in the analysis of soil health but it is very important as it illustrates the time period over which the soil returns to the equilibrium following the disturbance of auguring the borehole to install the soil sensor. The time required for this re-equilibration will vary depending on several factors, including the soil porosity and texture, which influence the rates of soil gas diffusion and advection.

Following the 12-h equilibration period, we can see that the soil temperature and soil CO<sub>2</sub> are positively correlated. As the soil temperature rises, so too does the metabolic activity of plant roots and microbes in the soil. As the aerobic soil metabolism is increased, so too is the production of CO<sub>2</sub> and, thus, the two data sets are strongly correlated over the observational period. Changes in the soil temperature generally follow changes in aboveground temperature, however, in this case, that relationship was obscured due to an insulating layer of snow that was present at the start of the observation period. Following a rise in the air temperature to above-freezing conditions, the snow cover melted late on February 15th, releasing liquid water into the soil which we observed as an increase in soil moisture peaking on February 16th in advance of subsequent rainfall later that day and on February 17th, which corresponded with a second increase in soil moisture on February 17th. Along with the snow-melt and rainfall induced increase in soil moisture, we also observed an increase in soil EC, indicating a likely flushing of dissolved salts into and through the soil.

### C. Evaluation of Wireless Communication Range

To evaluate the maximum wireless transmission range between a SHMU and the LoRaWAN gateway, an experiment was carried out in an open space (with partial line of sight) at the TPAC site and the weather conditions were as follows: the

TABLE III  
NOMENCLATURE

PDR	Packet Delivery Ratio
$T_{PR}$	Total number of packets delivered
$T_{PT}$	Total number of frames transmitted
$\bar{I}_{active}$	Average current consumption of the SHMU in active mode
$\bar{I}_{sleep}$	Average current consumption of the SHMU in sleep mode
$\bar{I}_{shmu}$	Average current consumption of the SHMU
$T_{active}$	Time period of the SHMU is in active mode
$T_{sleep}$	Time period of the SHMU is in sleep mode
$T_{warm}$	Warm up time of the $\text{CO}_2$ sensor
$I_{co2}$	Current consumption of the $\text{CO}_2$ sensor
$T$	Duration of one measurement cycle and is equal to $T_{active} + T_{sleep} + T_{warm}$
$(T_{oper})$	SHMU's operation time
$Q_{batt}$	Battery's capacity
$K$	Fraction of charge the Li-ion battery will deliver before its voltage drops below 3.4 V

air temperature ranges between  $-15^\circ\text{C}$  and  $17^\circ\text{C}$ , humidity ranges between 41% to 100%. In this experiment, the SHMU was moved to various distances from the gateway antenna ranging from 20 to 3486 m. The firmware of the SHMU was programmed to transmit 4000 frames at each distance and the corresponding PDR was calculated as follows:

$$\text{PDR} = T_{PR}/T_{PT}. \quad (1)$$

The measured PDR is shown in Fig. 16. Notably, a PDR of more than 85% is achieved up to a distance of 3422 m and at a transmission power of 10 dBm, spreading factor of 7. A PDR of 85% and above is acceptable for soil health analysis since the SHMUs transmit soil health data every 10 min, which is faster than the time scale of soil dynamics. Hence, missed data can be inferred from the available data.

From this experiment, it was found that soil health can be monitored without significant degradation in the signal up to a distance of 3422 m (for the conditions stated above). However, the wireless transmission distance will vary based on weather conditions. Longer distances can be achieved by increasing the transmission power upto 18.5 dBm, spreading factor up to 12, increasing the height of the LoRa gateway antenna or installing additional gateways.

#### D. Average Current Consumption of the SHMU

The current consumption of the SHMUs was evaluated with the aim of determining their operation time. Current consumption measurements were carried out with a Teros 12 sensor connected to the SHMU, LoRa radio module configured as follows: power level of 10 dBm, spreading factor of 7, coding rate of 4/5, and a bandwidth of 125 kHz, and the host microcontroller configured as follows: clock frequency of 8 MHz, supply voltage of 3.3 V, peripherals, such as UART0 and UART1, and GPIO controller. The current consumption of the SHMU was measured using the INA233 current monitor from Texas Instruments. The measured current is shown in Fig. 17. In the figure, the active and sleep modes of operation are clearly distinguishable. In the active mode, the microcontroller, LoRa radio, GPS module, and Teros 12 sensor are on. In the sleep mode, these components are placed in the power-down or sleep mode to reduce current consumption.

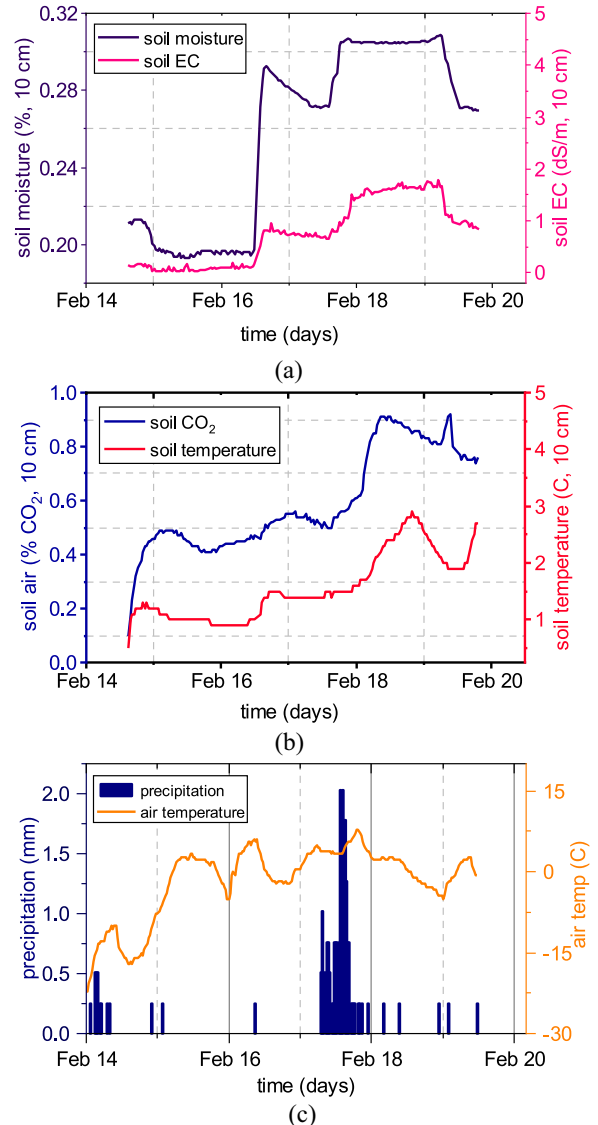


Fig. 15. Observational data of SHMU 9. (a) Soil gas  $\text{CO}_2$  percent concentration at 35-cm depth and soil temperature in  $^\circ\text{C}$  at 10-cm depth. (b) Soil moisture as volumetric percent at 10-cm depth and soil EC in  $\text{dS/m}$  at 10-cm depth. (c) Air temperature ( $^\circ\text{C}$ ) and precipitation (mm) data obtained via the TPAC weather station.

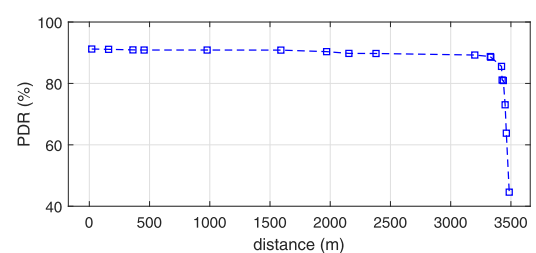


Fig. 16. Measured wireless transmission distance between a SHMU and the gateway at a transmission power level of 10 dBm, spreading factor of 7, and gateway antenna height of 7.9 m.

The average current consumption during  $\bar{I}_{active}$  and  $\bar{I}_{sleep}$  was calculated from the measured current and found to be equal to 34 mA and 328  $\mu\text{A}$ , respectively.

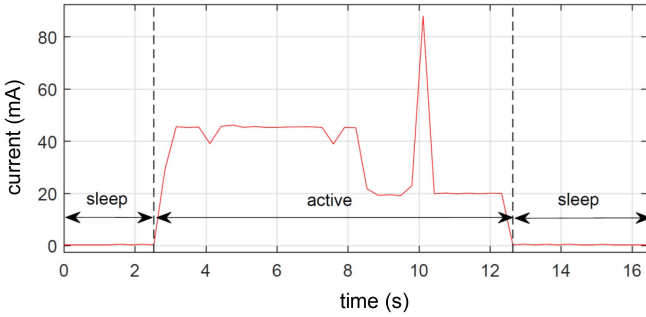


Fig. 17. Measured current consumption of the SHMU with a Teros 12 sensor connected to it and at a transmission power of 10 dBm.

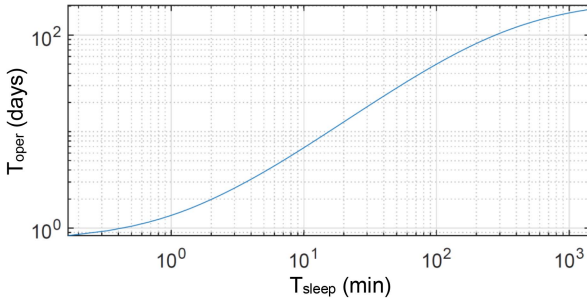


Fig. 18. Expected operation time of a SHMU powering a Teros 12 and CO<sub>2</sub> sensors as a function of sleep time.

The power consumption of the CO<sub>2</sub> sensor is 0.5 W and it draws a current of 135 mA from the Li-ion battery. Moreover, the CO<sub>2</sub> sensor requires a warm up time of at least 60 s before a reading can be made. Considering all these contributions,  $\overline{I_{\text{shmu}}}$  can then be estimated as follows:

$$\begin{aligned} \overline{I_{\text{shmu}}} &= \left( \frac{T_{\text{active}}}{T} \right) \overline{I_{\text{active}}} + \left( \frac{T_{\text{sleep}}}{T} \right) \overline{I_{\text{sleep}}} \\ &\quad + \left( \frac{T_{\text{warm}}}{T} \right) (\overline{I_{\text{co2}}} + \overline{I_{\text{sleep}}}). \end{aligned} \quad (2)$$

Using (2) and considering  $T_{\text{active}} = 10.1$  s,  $T_{\text{warm}} = 60$  s,  $\overline{I_{\text{co2}}} = 135$  mA, and  $T_{\text{sleep}} = 600$  s, it yields an overall average current consumption of 13 mA. If a SHMU is equipped with a Teros 12 sensor but not with a CO<sub>2</sub> sensor, the average current consumption drops to 939 μA.

The ( $T_{\text{oper}}$ ), defined as the time the battery can power the SHMU before needing to be recharged, can be estimated as follows:

$$T_{\text{oper}} = K \frac{Q_{\text{batt}}}{\overline{I_{\text{shmu}}}} \quad (3)$$

Considering  $Q_{\text{batt}} = 2500$  mAh,  $K = 0.85$ , and  $\overline{I_{\text{shmu}}} = 13$  mA, the SHMU's operation time is 163.46 hours or 6.8 days.

Depending on the soil monitoring needs,  $T_{\text{sleep}}$  can be adjusted to increase or decrease the sampling frequency of soil parameters. However, changing  $T_{\text{sleep}}$  also affects the average current consumption of the SHMU and, as a consequence, its operation time. Using (2) and (3), the operation time as a function of  $T_{\text{sleep}}$  can be found. Fig. 18 shows this relationship for a SHMU with both the Teros 12 and CO<sub>2</sub> sensors.

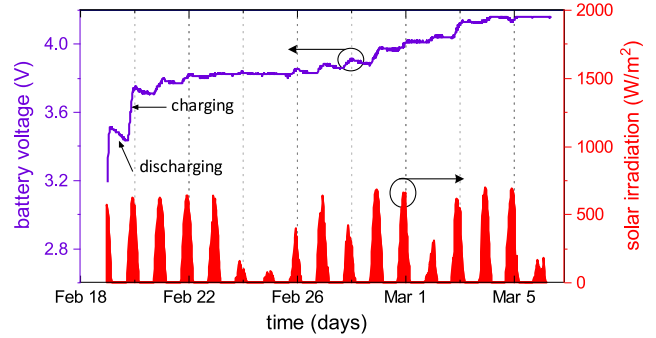


Fig. 19. Measured battery voltage of a SHMU and solar irradiance. For the voltage measurements, a Teros 12 sensor was connected to the SHMU and the SHMU was programmed to transmit data every 10 min at the maximum power of 18.5 dBm. Measurements were collected at the TPAC site.

Fig. 18 shows that an increase in  $T_{\text{sleep}}$  leads to an increase in the operation time. For instance, if  $T_{\text{sleep}}$  is set to 1 min, the operation time is 1.3 days but if  $T_{\text{sleep}}$  is increased to 60 min, the operation time increases to 33 days. This estimation does not take into account the battery's self-discharge, losses in the power management unit, or additional sensors connected to the SHMU, however, it shows that a 2500-mAh battery can power a SHMU with a Teros 12 and a CO<sub>2</sub> sensor for several days before needing to be recharged.

#### E. Battery Charging With Solar Power

The SHMU is equipped with a solar panel to recharge its onboard battery and enable long-term remote operation. To protect the SHMU from the elements, it was enclosed in a weatherproof case with IP67 rating. The weatherproof case is made out of durable polycarbonate material and its lid is made out of transparent fiberglass. The transparent lid protects the solar panel while letting light go through. However, due to its ultraviolet (UV) radiation-blocking rating, it also attenuates the solar irradiance that reaches the solar panel. To assess this attenuation, the current-versus-voltage (IV) curve of the solar panel was measured with and without the enclosure. From these curves, the maximum power generated by the solar panel was estimated for both cases. It was found that the enclosure's lid results in a 10% reduction in the maximum power generated by the solar panel. However, even with this reduction, the solar panel generated 345.8 mW of power (for a solar irradiance of 977 W/m<sup>2</sup>).

To estimate how long it will take to charge the SHMU's battery with solar power, the battery was discharged until its voltage dropped to 3.2 V. The SHMU was then deployed at the TPAC site for 14 days while its battery voltage was recorded at 10-min intervals. The solar power harvested by the solar panel and the BQ25505 energy harvesting chip fed the SHMU's electronic circuitry (including a Teros 12 sensor) and the surplus power went to charge the battery. The recorded battery voltage and the solar irradiance are shown in Fig. 19. The day and night cycles are clearly visible in the figure. The days with low solar irradiance levels corresponding to cloudy days. It can also be seen that the battery voltage increases during

TABLE IV  
PARTS COST OF A SHMU

Item	Cost in USD
Electronic components	44.26
Printed circuit board fabrication	10.77
Board assembly	35.97
GPS module (PAM-7Q)	22.40
915 MHz antenna	10.55
2,500 mAh Li-ion battery	14.95
Solar panel (MIKROE-651)	11.34
Weatherproof enclosure	10.10
Sensor expansion board	8.50
Cable glands, PVC pipe and fittings	10.50
<b>Total cost</b>	<b>179.34</b>

TABLE V  
IoT-SHM SYSTEM COSTS

Item	Cost in USD
LoRa gateway (Microchip)	360.00
Omni-directional 915 MHz antenna	250.00
Low-loss RF cable (15 m)	62.73
Teros 12 sensor	225.00
Vaisala GMP251 CO <sub>2</sub> sensor	717.00
Server computer (OptiPlex 5060 MFF)	862.79
<b>Total cost</b>	<b>2,477.52</b>

the day and decreases during the night. After 14 days, the battery voltage reached a voltage of 4.14 V demonstrating that the selected solar panel can provide enough energy to power a SHMU and charge its battery.

#### F. Cost of the IoT-SHM System

Table IV lists the parts needed to fabricate one SHMU along with their prices (if 30 SHMUs are fabricated). The cost to fabricate one SHMU is \$179 (without counting soil sensors). Table V lists the parts required to implement a full IoT-SHM system along with their prices. In our field deployment, we used nine SHMU's, eight of them were equipped with a Teros 12 sensor and one SHMU was equipped with both a Teros 12 and GMP251 CO<sub>2</sub> sensor. The total cost of our deployment was \$5667, out of which, 44.4% was for sensors. As the network is scaled up, the sensor cost starts to dominate the total cost. For instance, for a network deployment of 30 SHMUs, 30 Teros 12, and ten CO<sub>2</sub> sensors, the sensors account for 66.8% of the total cost.

#### G. Summary of Results

A summary of our experimental results is shown in Table VI, and are compared with the existing LoRa/LoRaWAN-based soil health monitoring systems reported in [42]–[45]. All these existing systems were deployed and tested in an agricultural field. However, the potential expansion of these systems was not validated. In [42], [43], and [45], the wireless coverage was evaluated and presented. In comparison, the achieved wireless range of the proposed system at 10 dBm is 80% higher than [42], 53% higher than [43], and 65% higher than [45], respectively. Additionally, the parameters, such as the current consumption and life expectancy, battery charging time, and the cost were studied and reported in the proposed system, whereas

TABLE VI  
SUMMARY OF RESULTS

Experiment	Result
1. Deployment and testing	A network was deployed at an agricultural field and soil health were analyzed using the soil health dashboard for 21 days.
2. Flexibility of the system	Evaluated by adding a Vaisala GMP251 CO <sub>2</sub> sensor alongside a Teros 12 sensor.
3. Ability to cover a large tracts of land	A wireless communication range of 3422 m was estimated at a transmission power of 10 dBm with 85% of packet delivery ratio.
4. Current consumption and life expectancy	A SHMU with a Teros 12 sensor as 939 μA, with a Teros 12 and a Vaisala sensor as 13 mA. At this rate, the on-board Li-ion battery is able to sustain a SHMU for several days.
5. Battery charging time	A 7 cm x 6.5 cm solar panel was able to fully charge the on-board battery in 14 days while supplying power to the SHMU.
6. Cost	Total cost of our deployment was 5,667 USD, includes: 8 SHMUs with a Teros 12 sensor, 1 SHMU with a Teros 12 & a CO <sub>2</sub> sensor, and a server computer.

these variables are not reported in [42]–[45]. Nevertheless, additional parameters such as sensitivity of a sensor, and the influence of soil moisture on received signal were studied and reported in [45]. These results and the features listed in Table I demonstrate that the developed system is better than the existing systems, and can be employed in remote field sites to study specific soil properties and other environmental parameters in real time.

## V. CONCLUSION

This article presented the development and use of an IoT system to monitor soil health using four dynamic properties (temperature, moisture, EC, and CO<sub>2</sub> concentration). All important aspects of the IoT system, such as soil health measurements and location data acquisition, long-range data transmission, data storage, data visualization, and a down-link channel for possible feedback control to improve crop production have been tested and validated successfully. A network consisting of nine SHMUs was deployed at an agricultural field site for several weeks and its performance in terms of soil sensing, wireless range, power consumption, life expectancy, and implementation cost was evaluated. Based on our experimental results, the proposed system is suitable for environmental monitoring and precision agriculture.

Future work in the area of the IoT-based soil health monitoring system includes: the generation of soil maps from sensor and geolocation data; interfacing additional sensors to study soil nitrate, phosphate, redox, pH, O<sub>2</sub>, and microbial activity; and the integration of machine learning algorithms to provide feedback with the aim of improving crop production.

## ACKNOWLEDGMENT

The authors express gratitude to Jay C. Young, Superintendent of the Throckmorton Purdue Agricultural Center, Purdue University, USA, for providing access to the

test site. Financial support for this work was provided by the Universidad Nacional de San Agustín (UNSA) through grant: Nexus Institute for Food, Energy, Water and the Environment.

## REFERENCES

- [1] R. Burt, *Soil Survey Field and Laboratory Methods Manual*, United States Dept. Agr., Nat. Resour. Conserv., Washington, DC, USA, Rep. 51, 2014.
- [2] E. K. Büemann *et al.*, “Soil quality—A critical review,” *Soil Biol. Biochem.*, vol. 120, pp. 105–125, May 2018.
- [3] J. W. Doran and M. R. Zeiss, “Soil health and sustainability: Managing the biotic component of soil quality,” *Appl. Soil Ecol.*, vol. 15, no. 1, pp. 3–11, 2000.
- [4] *Recommended Soil Health Indicators and Associated Laboratory Procedures. Soil Health Technical Note No. 450-03*, USDA Nat. Resour. Conserv. Serv., Washington, DC, USA, 2018.
- [5] H. Jenny, *Factors of Soil Formation. 281 PP.* New York, NY, USA: McGraw-Hill, 1941.
- [6] M. G. Kibblewhite, K. Ritz, and M. Swift, “Soil health in agricultural systems,” *Philos. Trans. Roy. Soc. B, Biol. Sci.*, vol. 363, no. 1492, pp. 685–701, 2008.
- [7] R. A. V. Rossel and A. B. McBratney, “Laboratory evaluation of a proximal sensing technique for simultaneous measurement of soil clay and water content,” *Geoderma*, vol. 85, no. 1, pp. 19–39, 1998.
- [8] B. Kuang, H. S. Mahmood, M. Z. Quaishi, W. B. Hoogmoed, A. M. Mouazen, and E. J. van Henten, “Sensing soil properties in the laboratory, in situ, and on-line: A review,” in *Advances in Agronomy*, vol. 114. Amsterdam, The Netherlands: Elsevier, 2012, pp. 155–223.
- [9] M. Futagawa, T. Iwasaki, H. Murata, M. Ishida, and K. Sawada, “A miniature integrated multimodal sensor for measuring pH, EC and temperature for precision agriculture,” *Sensors*, vol. 12, no. 6, pp. 8338–8354, 2012.
- [10] S. J. Ramson, S. Vishnu, and M. Shanmugam, “Applications of Internet of Things (IoT): An overview,” in *Proc. IEEE 5th Int. Conf. Devices Circuits Syst. (ICDCS)*, 2020, pp. 92–95.
- [11] R. K. Pathinarupothi, P. Durga, and E. S. Rangan, “IoT-based smart edge for global health: Remote monitoring with severity detection and alerts transmission,” *IEEE Internet Things J.*, vol. 6, no. 2, pp. 2449–2462, Apr. 2019.
- [12] G. Fortino, W. Russo, C. Savaglio, M. Viroli, and M. C. Zhou, “Modeling opportunistic IoT services in open IoT ecosystems,” in *Proc. 18th Workshop From Objects Agents (WOA)*, 2017, pp. 90–95.
- [13] E. Municio *et al.*, “Continuous athlete monitoring in challenging cycling environments using IoT technologies,” *IEEE Internet Things J.*, vol. 6, no. 6, pp. 10875–10887, Dec. 2019.
- [14] S. Gao, X. Zhang, C. Du, and Q. Ji, “A multichannel low-power wide-area network with high-accuracy synchronization ability for machine vibration monitoring,” *IEEE Internet Things J.*, vol. 6, no. 3, pp. 5040–5047, Jun. 2019.
- [15] Z. Huang, Q. Chen, L. Zhang, and X. Hu, “Research on intelligent monitoring and analysis of physical fitness based on the Internet of Things,” *IEEE Access*, vol. 7, pp. 177297–177308, 2019.
- [16] G. Yang *et al.*, “IoT-based remote pain monitoring system: From device to cloud platform,” *IEEE J. Biomed. Health Inform.*, vol. 22, no. 6, pp. 1711–1719, Nov. 2018.
- [17] M. E. E. Alahi, N. Pereira-Ishak, S. C. Mukhopadhyay, and L. Burkitt, “An Internet-of-Things enabled smart sensing system for nitrate monitoring,” *IEEE Internet Things J.*, vol. 5, no. 6, pp. 4409–4417, Dec. 2018.
- [18] S. J. Ramson, D. J. Moni, S. Vishnu, T. Anagnostopoulos, A. A. Kirubaraj, and X. Fan, “An IoT-based bin level monitoring system for solid waste management,” *J. Mater. Cycles Waste Manag.*, pp. 1–10, Nov. 2020.
- [19] S. Ding and X. Wang, “Medical remote monitoring of multiple physiological parameters based on wireless embedded Internet,” *IEEE Access*, vol. 8, pp. 78279–78292, 2020.
- [20] S. Vishnu, S. R. J. Ramson, and R. Jegan, “Internet of medical things (IoMT)—An overview,” in *Proc. IEEE 5th Int. Conf. Devices Circuits Syst. (ICDCS)*, Coimbatore, India, 2020, pp. 101–104.
- [21] F. M. Hopkins, M. S. Torn, and S. E. Trumbore, “Warming accelerates decomposition of decades-old carbon in forest soils,” *Proc. Nat. Acad. Sci.*, vol. 109, no. 26, pp. E1753–E1761, 2012.
- [22] Z. S. Brecheisen, C. W. Cook, P. R. Heine, J. Ryang, and D. D. Richter, “Development and deployment of a field-portable soil O<sub>2</sub> and CO<sub>2</sub> gas analyzer and sampler,” *PLoS ONE*, vol. 14, no. 8, 2019, Art. no. e0220176.
- [23] S. A. Billings *et al.*, “Loss of deep roots limits biogenic agents of soil development that are only partially restored by decades of forest regeneration,” *Elementa Sci. Anthropocene*, vol. 6, no. 1, p. 34, 2018.
- [24] C. B. Hedley and I. J. Yule, “Soil water status mapping and two variable-rate irrigation scenarios,” *Precis. Agr.*, vol. 10, no. 4, pp. 342–355, 2009.
- [25] M. E. Moshia, R. Khosla, J. G. Davis, D. G. Westfall, and K. Doesken, “Precision manure management on site-specific management zones: Topsoil quality and environmental impact,” *Commun. Soil Sci. Plant Anal.*, vol. 46, no. 2, pp. 235–258, 2015.
- [26] R. E. Sweeney and G. T. Ririe, “Temperature as a tool to evaluate aerobic biodegradation in hydrocarbon contaminated soil,” *Groundwater Monitor. Remediation*, vol. 34, no. 3, pp. 41–50, 2014.
- [27] O. Adeyemi, I. Grove, S. Peets, and T. Norton, “Advanced monitoring and management systems for improving sustainability in precision irrigation,” *Sustainability*, vol. 9, no. 3, p. 353, 2017.
- [28] S. R. J. Ramson and D. J. Moni, “Wireless sensor networks based smart bin,” *Comput. Electr. Eng.*, vol. 64, pp. 337–353, Nov. 2017.
- [29] H. R. Bogena, M. Herbst, J. A. Huisman, U. Rosenbaum, A. Weuthen, and H. Vereecken, “Potential of wireless sensor networks for measuring soil water content variability,” *Vadose Zone J.*, vol. 9, no. 4, pp. 1002–1013, 2010.
- [30] B. Kerkez, S. D. Glaser, R. C. Bales, and M. W. Meadows, “Design and performance of a wireless sensor network for catchment-scale snow and soil moisture measurements,” *Water Resour. Res.*, vol. 48, no. 9, pp. 1–18, 2012.
- [31] B. Majone *et al.*, “Wireless sensor network deployment for monitoring soil moisture dynamics at the field scale,” *Procedia Environ. Sci.*, vol. 19, pp. 426–435, Jul. 2013.
- [32] M. T. Lazarescu, “Design of a WSN platform for long-term environmental monitoring for IoT applications,” *IEEE J. Emerg. Sel. Topics Circuits Syst.*, vol. 3, no. 1, pp. 45–54, Mar. 2013.
- [33] S. Khrijji, D. El Houssainei, M. W. Jmal, C. Viehweger, M. Abid, and O. Kanoun, “Precision irrigation based on wireless sensor network,” *IET Sci. Meas. Technol.*, vol. 8, no. 3, pp. 98–106, 2014.
- [34] Z. Li *et al.*, “Practical deployment of an in-field soil property wireless sensor network,” *Comput. Stand. Interfaces*, vol. 36, no. 2, pp. 278–287, 2014.
- [35] P. Spachos and D. Hatzinakos, “Real-time indoor carbon dioxide monitoring through cognitive wireless sensor networks,” *IEEE Sensors J.*, vol. 16, no. 2, pp. 506–514, Jan. 2016.
- [36] U. K. Madhura, P. Akshay, A. J. Bhattacharjee, and G. S. Nagaraja, “Soil quality management using wireless sensor network,” in *Proc. 2nd Int. Conf. Comput. Syst. Inf. Technol. Sustain. Solution (CSITSS)*, Bangalore, India, 2017, pp. 1–5.
- [37] G. Villalba *et al.*, “A networked sensor system for the analysis of plot-scale hydrology,” *Sensors*, vol. 17, no. 3, p. 636, 2017.
- [38] R. G. Vieira, A. M. Da Cunha, L. B. Ruiz, and A. P. De Camargo, “On the design of a long range WSN for precision irrigation,” *IEEE Sensors J.*, vol. 18, no. 2, pp. 773–780, Jan. 2017.
- [39] J. J. Estrada-López, A. A. Castillo-Atoche, J. Vázquez-Castillo, and E. Sánchez-Sinencio, “Smart soil parameters estimation system using an autonomous wireless sensor network with dynamic power management strategy,” *IEEE Sens. J.*, vol. 18, no. 21, pp. 8913–8923, Nov. 2018.
- [40] A. Roy and K. Barman, “An adaptive technique for soil moisture control and nutrient monitoring using wireless sensor network,” *Think India J.*, vol. 22, no. 17, pp. 1558–1564, 2019.
- [41] Y. Kuang, Y. Shen, L. Lu, and G. Li, “Farmland monitoring system based on cloud platform,” in *Proc. IEEE 8th Joint Int. Inf. Technol. Artif. Intell. Conf. (ITAIC)*, Chongqing, China, 2019, pp. 335–339.
- [42] A. F. Rachmani and F. Y. Zulkifli, “Design of IoT monitoring system based on LoRa technology for starfruit plantation,” in *Proc. TENCON IEEE Region 10 Conf.*, Jeju, South Korea, 2018, pp. 1241–1245.
- [43] X. Zhang, M. Zhang, F. Meng, Y. Qiao, S. Xu, and S. Hour, “A low-power wide-area network information monitoring system by combining NB-IoT and LoRa,” *IEEE Internet Things J.*, vol. 6, no. 1, pp. 590–598, Feb. 2019.
- [44] Y. Jia, “LoRa-based WSNs construction and low-power data collection strategy for wetland environmental monitoring,” *Wireless Pers. Commun.*, vol. 114, pp. 1533–1555, May 2020.
- [45] F. Deng, P. Zuo, K. Wen, and X. Wu, “Novel soil environment monitoring system based on RFID sensor and LoRa,” *Comput. Electron. Agr.*, vol. 169, Feb. 2020, Art. no. 105169.
- [46] Y. Mehmood, F. Ahmad, I. Yaqoob, A. Adnane, M. Imran, and S. Guizani, “Internet-of-Things-based smart cities: Recent advances and challenges,” *IEEE Commun. Mag.*, vol. 55, no. 9, pp. 16–24, Sep. 2017.

- [47] B. Citoni, F. Fioranelli, M. A. Imran, and Q. H. Abbasi, "Internet of Things and LoRaWAN-enabled future smart farming," *IEEE Internet Things Mag.*, vol. 2, no. 4, pp. 14–19, Dec. 2019.
- [48] D. Davcev, K. Mitreski, S. Trajkovic, V. Nikolovski, and N. Koteli, "IoT agriculture system based on LoRaWAN," in *Proc. 14th IEEE Int. Workshop Factory Commun. Syst. (WFCS)*, Imperia, Italy, 2018, pp. 1–4.
- [49] T. N. Gia, L. Qingqing, J. P. Queralta, Z. Zou, H. Tenhunen, and T. Westerlund, "Edge AI in smart farming IoT: CNNs at the edge and fog computing with LoRa," in *Proc. IEEE AFRICON*, 2019, pp. 1–6.
- [50] N. A. Alrajeh, M. Bashir, and B. Shams, "Localization techniques in wireless sensor networks," *Int. J. Distrib. Sens. Netw.*, vol. 9, no. 6, 2013, Art. no. 304628.
- [51] D. R. Smith, G. Hernandez-Ramirez, S. D. Armstrong, D. L. Bucholtz, and D. E. Stott, "Fertilizer and tillage management impacts on non-carbon-dioxide greenhouse gas emissions," *Soil Sci. Soc. Amer. J.*, vol. 75, no. 3, pp. 1070–1082, 2011.
- [52] B. Stipešević and E. J. Kladivko, "Effects of winter wheat cover crop desiccation times on soil moisture, temperature and early maize growth," *Plant Soil Environ.*, vol. 51, no. 6, pp. 255–261, 2005.
- [53] M. Li *et al.*, "A new dynamic wetness index (DWI) predicts soil moisture persistence and correlates with key indicators of surface soil geochemistry," *Geoderma*, vol. 368, Jun. 2020, Art. no. 114239.
- [54] R. Sørensen, U. Zinko, and J. Seibert, "On the calculation of the topographic wetness index: Evaluation of different methods based on field observations," *Hydrol. Earth Syst. Sci.*, vol. 10, no. 1, pp. 101–112, 2006.
- [55] J. P. Molin and G. D. C. Faulin, "Spatial and temporal variability of soil electrical conductivity related to soil moisture," *Scientia Agricola*, vol. 70, no. 1, pp. 01–05, 2013.
- [56] R. Zhang and B. J. Wienhold, "The effect of soil moisture on mineral nitrogen, soil electrical conductivity, and pH," *Nutrient Cycling Agroecosyst.*, vol. 63, nos. 2–3, pp. 251–254, 2002.
- [57] M. N. Nielsen, A. Winding, and S. Binnerup, *Microorganisms as Indicators of Soil Health*. Roskilde, Denmark: Nat. Environ. Res. Inst., 2002.



**Zachary Brecheisen** received B.A. degree from New Mexico State University, New Mexico, USA, in 2012, and the Ph.D. from Duke University, North Carolina, USA, in 2018.

He is a "critical-zonist" interested in how ecosystems respond to human disturbance, especially agriculture and old-field succession. He pairs remote sensing with field observations to enhance soils and forestry investigations. His academic training from undergraduate (NMSU) through graduate school (Duke University) into Postdoctoral Research

(Purdue University) has been cross-disciplinary with collaborators from earth sciences, social sciences, and the humanities via the critical zone observatory network and the Arequipa Nexus Institute, Purdue University. His research includes land-cover classification, geomorphic terrain analyzes, gas chromatography, 3-D printing, x-ray computed tomography, and data logging environmental sensors.



**Erika J. Foster** received the Ph.D. in Ecology from Colorado State University, Colorado, USA, in 2018.

He is a Soil Agroecologist, researching the response of soil biogeochemistry to management. She quantifies the accumulation and stabilization of organic matter under agricultural systems and plant-soil-microbe interactions. She is an Investigator with the Arequipa Nexus Institute, Purdue University, West Lafayette, IN, USA. She works within a massive irrigation project in a hyper-arid region of southern Peru to develop an agricultural chronose-

quence of carbon development. She compiled and designed a soil health field test kit for small shareholder farmers of the region to combine with rapid scans of elemental content (pXRF) and organic carbon (Vis-NIR) to contribute to digital soil maps.



**S. R. Jino Ramson** (Member, IEEE) received the B.Eng. degree in electronics and communication engineering from Anna University, Chennai, India, in 2007, and the M.Tech. degree in networks and Internet engineering, and the Ph.D. degree in electronics and communication engineering from Karunya University, Coimbatore, India, in 2010 and 2017, respectively.

He served as a Postdoctoral Research Assistant with the School of Engineering Technology, Purdue University, West Lafayette, IN, USA, where he is a Postdoctoral Research Associate with the Department of Earth, Atmospheric, and Planetary Sciences. Apart from his research experiences, he has served as a Faculty for a period of around nine years and taught courses in the field of Internet of Things, computer networks, electronic devices and circuits, signal processing, and embedded systems. His research interest is to develop real-time IoT systems in various disciplines, such as precision agriculture, environmental monitoring, solid-waste management, and human healthcare.



**Cliff T. Johnston** received the B.S. degree in chemistry and the Ph.D. degree in soil science from the University of California at Riverside, Riverside, CA, USA, in 1979 and 1983, respectively.

He received additional training as a Postdoctoral Fellow with Los Alamos National Laboratory, Los Alamos, NM, USA. He is a Professor of Soil Chemistry with the Departments of Agronomy and Earth, Atmospheric, and Planetary Sciences, Purdue University, West Lafayette, IN, USA. He studies mineral-organic and mineral-water interactions in the context of biosphere science. He teaches courses in soil chemistry, soil biogeochemistry, and environmental science. Research topics include protection of soil organic matter, fate and transport of toxic chemicals, and emissions of greenhouse gases from agricultural landscapes.



**Walter D. León-Salas** (Member, IEEE) received the B.S. degree in electronic engineering from the Universidad Nacional de San Agustín, Arequipa, Peru, in 1996, and the M.S. and Ph.D. degrees in electrical engineering from the University of Nebraska-Lincoln, Lincoln, NE, USA, in 2001 and 2006, respectively.

He is currently an Associate Professor with the School of Engineering Technology, Purdue University, West Lafayette, IN, USA. His research interests include energy harvesting, wireless sensors, CMOS imaging and data compression. He has published over 70 journal and conference papers in the above areas.

Dr. León-Salas received the CAREER Award from the National Science Foundation in 2011.



**Darrell G. Schulze** received the B.S. and M.S. degrees from Texas A&M University, Texas, USA, in 1975 and 1977, respectively, and the Ph.D. degrees from the Technical University of Munich, Munich, Germany, in 1982.

He is a Professor of Soil Science with Purdue University, West Lafayette, IN, USA. He teaches a field-based course titled, soils and landscapes, for which he developed an innovative teaching with-maps approach that is used in various courses at Purdue and elsewhere. He leads the development of

soil explorer, a soil data visualization platform that is available as an app for iOS and Android and as a website (SoilExplorer.net). His work with the Arequipa Nexus Institute is primarily focused on visualizing soil and landscape data. His research and teaching interests span various aspects of soil science, including pedology, digital soil mapping, mineralogy, soil chemistry, and international agriculture.



**Timothy Filley** received the B.S. degree in chemistry from the Loyola University of Chicago, Chicago, IL, USA, in 1990, and the Ph.D. degree in isotope geochemistry from the Pennsylvania State University, State College, PA, USA, in 1997.

He is a Professor of Stable Isotope Biogeochemistry with the Department of Earth, Atmospheric, and Planetary Sciences, Purdue University, West Lafayette, IN, USA, where he is the Director of the Center for the Environment and the U.S.-China EcoPartnership for Environmental

Sustainability. Broadly, Using natural abundance and highly enriched stable isotopes and biomarker tools his group investigates how perturbations to ecosystems interact with soil and microbial properties to stabilize or destabilize soil organic matter. His research focuses on the fundamental processes controlling the cycling of carbon and nitrogen in soil, litter, and streams within natural and managed ecosystems, and the implications of such biogeochemistry to the fate of emerging pollutants.



**Juan A. Lopa Bolívar** received the bachelor's degree from the National University of San Agustín in Arequipa, Arequipa, Peru, in 1986, and the master's degree from the Graduate School of the National University of San Agustín, Arequipa, through an agreement with the University of Surrey, Guildford, U.K., in 1990, and the Doctoral degree in environmental sciences and technology from the Graduate School of the National University of San Agustín de Arequipa, Arequipa, by agreement with the Universidad Católica del Norte, Antofagasta,

Chile, in 2009.

He is a Senior Researcher, appointed in the Professional School of Chemistry, College of Natural and Formal Sciences with the National University of San Agustín Arequipa.



**Rahim Rahimi** (Senior Member, IEEE) received the Ph.D. degree in electrical and computer engineering from Purdue University, West Lafayette, IN, USA, in 2017.

His work has been featured in various news media, including science nation, Science360, the computer world, and science. He has led research teams on multiinstitutional research endeavors with a focus on developing scalable manufacturing processes of flexible electronic devices that can empower technologies for health-care, and environmental monitoring.

His research has explored development of innovative, scalable, multifunctional, microsystem platforms for medical applications, with emphasis on smart wearable and autonomous devices for wound monitoring and therapy.



**Martín Juan Carlos Villalta Soto** received the bachelor's degree in agricultural sciences in and the master's degree in Agroecology from the National University San Agustín de Arequipa (UNSA), Arequipa, Peru, in 1988 and 2007, respectively, and the postgraduation degree in edaphology in 1996.

In 1989, he was title of Agricultural Engineer. He began as the Head of Edaphology Practices, UNSA in 1989, where he is a Main Professor. He teaches edaphology, soil fertility, soil management, and conservation. He has participated in the following projects: Agricultural Research and Extension in the High Andean zones in 1989; Collection of Soil Monoliths INIAA-ISRIC in 1991; Agricultural Soil Analysis Service from 1990 to 1995 School of Agronomy, UNSA and Assessment-Vulnerability and soil health UNSA-Purdue from 2018 to 2020.



**Mauricio Postigo Málaga** (Member, IEEE) received the B.S. degree in electronic engineering from the Universidad Nacional de Ingeniería, Lima, Peru, in 1989, and the M.Sc. degree in telecommunication engineering from the Universidad Nacional de San Agustín de Arequipa, Arequipa, Peru, in 2010, where he is currently pursuing the Ph.D. degree.

Since 1989, he has been a Senior Professor with the School of Electronic and Telecommunication Engineering, Universidad Nacional de San Agustín de Arequipa. He has been the Project Manager and an External Consultant in research and development projects in telecommunications. His research interests include wireless sensor networks and wireless and fiber optic communications systems.